Type-II core/shell nanoparticle induced photorefractivity

Xiangping Li,[1] Joel Van Embden,[1] Richard A. Evans,[2] and Min Gu[1,a)]
[1]*Centre for Micro-Photonics, Faculty of Engineering and Industrial Sciences, Swinburne University of Technology, Hawthorn, Victoria 3122, Australia*
[2]*CSIRO Materials Science and Engineering, Clayton 3168, Australia*

(Received 13 April 2011; accepted 6 May 2011; published online 8 June 2011)

We demonstrate engineering the photocharge generation efficiency of nanoparticles on the nanometer scale by using a type-II band-gap structure. Compared to bare CdSe cores, the dispersion of type-II core/shell nanoparticles in photorefractive polymer led to an average 100% increase in photocurrents. An improvement to the refractive-index construction time, and a near 100% enhancement to the two beam coupling net-gain coefficients and four-wave mixing internal diffraction efficiencies have been achieved at moderate biases. © *2011 American Institute of Physics*. [doi:10.1063/1.3596437]

Photorefractive polymer composites have been identified as key to next generation green photonics owing to the fact that they exhibit reversible volumetric refractive-index modulation, compositional flexibility, and are synthesized with relative ease. These attributes make these composite polymer based materials attractive to a wide range of applications including optical data storage,[1] dynamic holography,[1,2] optical image processing, and three-dimensional displays.[3,4] Photorefractivity arises when charge carriers, photogenerated by a spatially inhomogeneous irradiation pattern, are separated and trapped to produce a non-uniform space charge distribution.[5] In this regard, dispersing semiconductor quantum dots (QDs)[6,7] into photorefractive polymers as photosensitizers has attracted much research interest over the past decade.[8–13]

So far the reported photorefractive performances of almost all QD-polymer composites have been low with response times of several seconds and diffraction efficiencies less than one percent at modest biases.[8,14–16] Limited success has been reported by growing a wide band gap shell material on the surface of core QDs. While these type-I core/shell QDs led to an enhanced refractive-index modulation, it came at the cost of slow response times.[17] This may be attributed to the difficulty in separating the charges, which must overcome the large potential barrier constructed between QD core and the shell.[15,17] In principle type-II heterostructure QDs should overcome the inherent pitfalls of both core QDs and type-I core/shell heterostructures. However, type-II core/shell nanoparticle induced photorefractivity has never been explored. In this letter, we report on the enhanced photorefractive performance induced by type-II CdSe/CdTe core/shell QDs.

In the case of a type-II band-gap alignment the valence and conduction band edges of the shell materials are either higher or lower than those of the respective band-edges in the core QD.[18–20] As a consequence, after excitation the carriers thermally relax into a spatially separated state where either the electron or hole is delocalized to the surface of the heterostructure, as illustrated in Figs. 1(a) and 1(b). This band architecture facilitates quick and efficient separation of the electron–hole pair after excitation.[18] In such a case, free carrier generation is expected to be enhanced, which can then be employed as a means to increase the photorefractive performance of a given device, as illustrated in Fig. 1(c).

CdSe core particles were synthesized following a well established method.[21] Growing the CdTe shell accomplished using the successive ionic layer adsorption and reaction method.[22–25] Figure 2 shows the absorption and photoluminescence (PL) spectra of the QDs before and after shell deposition. The PL peak redshifted almost 0.4 eV from 1.95 to 1.57 eV after four injections of Cd and Te precursors. The large spectral redshift is a direct consequence of the reduced quantum confinement in the new heterostructure. It should be noted that the PL efficiency after shell deposition was drastically reduced to about one tenth that of the core QD; owing to the enhanced charge separation in the excited state. From knowledge of the initial mean CdSe core size transmission electron microscopy (TEM) measurements of the final CdSe/CdTe core/shells, as shown in Fig. 2 inset, highlight that the

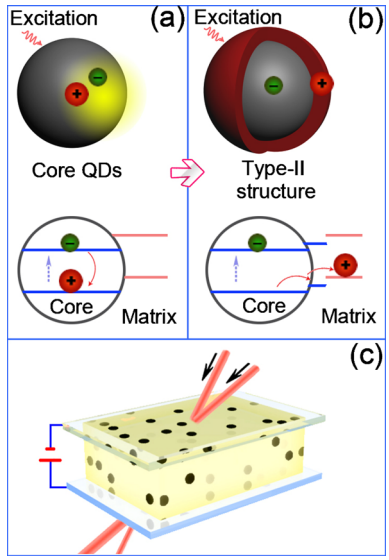

FIG. 1. (Color online) (a) Quantum confinement leads to an enhanced recombination of photogenerated electron–hole pairs inside a core QD. (b) Photocharge generation is enhanced in a type-II core/shell structure QD by separating electron–hole pairs and delocalizing them in the core and shell region, respectively. (c) Schematic of the device architecture used to measure photorefractivity.

a)Author to whom correspondence should be addressed. Electronic mail: mgu@swin.edu.au.

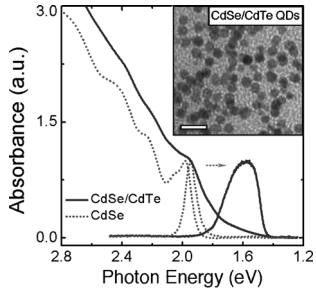

FIG. 2. Absorption and PL spectra of CdSe core QDs (dotted line) and CdSe/CdTe type-II QDs (solid line) in chloroform. The inset shows a TEM of the CdSe/CdTe QDs. The scale bar is 20 nm.

CdTe shell deposition is homogeneous with a thickness around ~0.7 nm.

The core and core/shell QDs were thoroughly purified via successive washings and ligand exchanged with 4-methylbenzene thiol. At this time the QDs were then able to be dispersed into the appropriate polymer blends and the devices fabricated. To measure the photoelectrical properties of the QDs both the CdSe cores and the CdSe/CdTe type-II QDs were dispersed into the polymer blends [poly(vinyl carbazole):ethyl carbazole (ECZ):4-diethylaminobenzylidene-malononitrile (DABM) at the ratio of 54 mg:16 mg:30 mg][25] at a concentration to yield a similar absorbance at the excitation wavelength of 1.96 eV. The absorption spectra of the prepared films together with that of a control sample without QDs are shown in Fig. 3(a). It should be noted that the QD-polymer composites appeared optical clear with no visible scattering. The measured absorbances, α, of the control sample, CdSe-sensitized and CdSe/CdTe-sensitized samples are 0.34 cm^{-1}, 4.50 cm^{-1}, and 5.05 cm^{-1} at the excitation wavelength, respectively [see arrow in Fig. 3(a)]. The photocurrent measurement of the as-prepared samples with thickness of 120 ± 10 μm at the irradiance intensity of 3.6 mW/cm^2 is shown in Fig. 3(b). As the field strength is increased the photocurrent of the QD-polymer composites increases dramatically. It can be immediately seen that, compared to the CdSe-sensitized sample, the CdSe/CdTe sample has a greater sensitivity to the external field, as expected from the type-II band-edge alignment. At 54 V/μm the sample sensitized by CdSe/CdTe has 250% more photocurrent than the CdSe-sensitized sample. On average, across the entire electric field range investigated here, the photocurrent

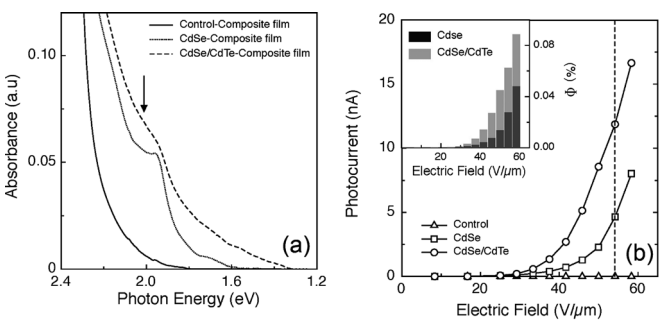

FIG. 3. (a) Absorbance of the of the control sample (solid line), CdSe sensitized sample (dotted line), and CdSe/CdTe sensitized sample (dashed line). The arrow indicates the excitation energy. (b) Photocurrent as a function of the external electric field for the control sample (triangles), CdSe sensitized (squares), and CdSe/CdTe sensitized (circles) polymer composites. The inset shows a plot of the photocharge generation quantum efficiencies in these samples.

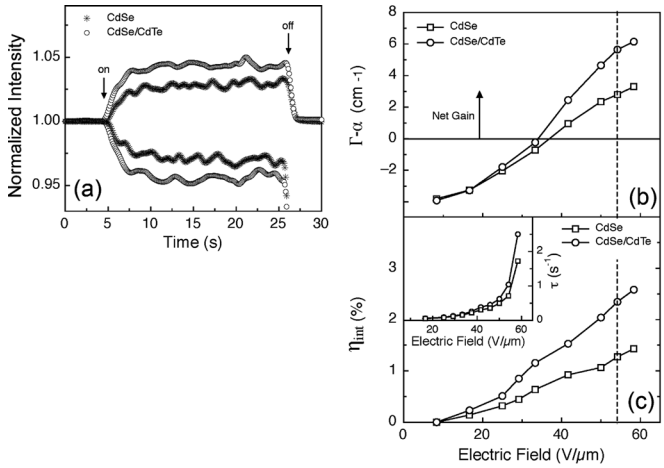

FIG. 4. (a) Transmitted intensities of the two beams in the CdSe sensitized (stars) and CdSe/CdTe sensitized (open circles) samples at a bias of 54 V/μm. One of the two beams is switched on at 5 s and turned off at 26 s. (b) Plots of 2BC net-gain coefficients as a function of the applied electric field. (c) FWM internal diffraction efficiencies as a function of the applied electric field. Squares and circles are data for CdSe sensitized and CdSe/CdTe sensitized composites, respectively. The inset shows a plot of the refractive-index construction time as a function of the applied electric field.

from the CdSe/CdTe-sensitized sample was found to be approximately 100% higher compared to the CdSe-sensitized sample. It should be noted that no detectable photocurrent (or photorefractivity) was observed in the control sample.

The quantum efficiency for photocharge generation can be obtained as[26]

$$\phi = J_{ph}\frac{hc}{I\lambda e\alpha d}, \tag{1}$$

where h is Planck's constant, c is the speed of the light, e is the fundamental unit of charge, α is the absorption coefficient, and d is the thickness of the sample. The inset of Fig. 3(b) shows a plot of the quantum efficiency for photocharge generation as a function of the external bias for the CdSe and CdSe/CdTe sensitized samples. It can be seen that the photocharge generation efficiency when employing type-II QDs is on average two to three times greater than bare core QDs over the total range of field strengths investigated here. Given that the absorption coefficient (α) at the band-edge was almost identical (within 10%), the enhancement in charge generation efficiency can be confidently attributed to the efficient electron–hole pair separation facilitated by the type-II QDs.

To demonstrate the consequent improvement in the strength of the refractive-index modulation, both two beam coupling (2BC) and four-wave mixing (FWM) experiments were conducted in a tilted geometry with incident angles of the two beams at 30° and 60° in air, respectively.[12] The characteristic asymmetrical energy transfer between the two p-polarized beams with intensities of 200 mW/cm^2 and 400 mW/cm^2, respectively, is a measurement of the photorefractive performance. The transmitted intensities of the two beams for the core QD and the type-II core/shell QD sensitized samples are shown in Fig. 4(a). The net-gain coefficients, Γ-α, are plotted as a function of the external electric field strength in Fig. 4(b). At a bias of 54 V/μm the net gain coefficients in CdSe and CdSe/CdTe sensitized samples were found to be 2.8 cm^{-1} and 5.7 cm^{-1}, respectively. This corresponds to an approximate 100% enhancement.

According to $\Gamma \sim \Delta n \sin\theta$,[27] where θ is the phase shift between the constructed refractive-index grating with the illumination grating, the strength of the refractive-index modulation increased by 47% (provided that the phase shifts were equal in two samples). For very small changes in the refractive index modulation (Δn) the internal diffraction efficiency, η_{int}, is proportional to Δn.[2,27] As a result small increases in refractive-index modulation can lead to a significant improvements to the internal diffraction efficiency. This was in fact confirmed by a FWM measurement [shown in Fig. 4(c)], where the intensity of the probe beam was kept low at 5.8 mW/cm^2. It can be immediately seen that the overall diffraction efficiency in the CdSe/CdTe sensitized composite is higher compared to the CdSe sensitized composite. At a bias of 54 $V/\mu m$ the internal diffraction efficiencies achieved in the CdSe and CdSe/CdTe sensitized samples were found to be 1.27% and 2.34%, respectively, which yields an 84% overall enhancement and corresponds to an 36% enhancement in refractive-index modulation. This result is consistent with the 2BC measurement, confirming that high refractive-index modulations are possible in composites sensitized by type-II core/shell QDs. In addition, faster construction of the refractive-index gratings were observed using type-II QDs [inset of Fig. 4(c)]. The response times over the entire investigated electric field range are faster in the CdSe/CdTe sensitized sample compared to the CdSe sensitized sample. This result may again be attributed to enriched free carrier generation. In particular, the characteristic refractive-index construction time was reduced from 580 to 400 ms at a bias of 58 $V/\mu m$.

In conclusion, we have demonstrated enhanced photorefractivity by employing type-II CdSe/CdTe QDs. The optimized type-II core/shell QDs led to efficient separation of electron–hole pairs and consequently led to an average 100% increase in photocurrent compared to CdSe cores. A near 100% enhanced 2BC net gain coefficient and FWM diffraction efficiency has been achieved at moderate biases. The results presented here demonstrate that engineering charge separation on the nanoscale is a promising means to improve photorefractive device performance.

Min Gu thanks the Australian Research Council for its funding support through Grant No. FL100100099. Min Gu and Xiangping Li thank the Australian Research Council for its funding support through Grant No. DP110101422. The authors would also like to thank Dr. James Chon for fruitful discussions. Xiangping Li and Joel Van Embden contributed equally to this work.

[1] K. Meerholz, B. L. Volodin, Sandalphon, B. Kippelen, and N. Peyghambarian, Nature (London) **371**, 497 (1994).
[2] B. Kippelen, S. R. Marder, E. Hendrickx, J. L. Maldonado, G. Guillemet, B. L. Volodin, D. D. Steele, Y. Enami, Sandalphon, Y. J. Yao, J. F. Wang, H. Rockel, L. Erskine, and N. Peyghambarian, Science **279**, 54 (1998).
[3] S. Tay, P. A. Blanche, R. Voorakaranam, A. V. Tun, W. Lin, S. Rokutanda, T. Gu, D. Flores, P. Wang, G. Li, P. St Hilaire, J. Thomas, R. A. Norwood, M. Yamamoto, and N. Peyghambarian, Nature (London) **451**, 694 (2008).
[4] P. A. Blanche, A. Bablumian, R. Voorakaranam, C. Christenson, W. Lin, T. Gu, D. Flores, P. Wang, W. Y. Hsieh, M. Kathaperumal, B. Rachwal, O. Siddiqui, J. Thomas, R. A. Norwood, M. Yamamoto, and N. Peyghambarian, Nature (London) **468**, 80 (2010).
[5] B. E. A. Saleh and M. C. Teich, *Fundamentals of Photonics* (Wiley, New York, 2007).
[6] A. P. Alivisatos, Science **271**, 933 (1996).
[7] W. E. Moerner and S. M. Silence, Chem. Rev. (Washington, D.C.) **94**, 127 (1994).
[8] C. Fuentes-Hernandez, D. J. Suh, B. Kippelen, and S. R. Marder, Appl. Phys. Lett. **85**, 534 (2004).
[9] J. G. Winiarz, L. Zhang, M. Lal, C. S. Friend, and P. N. Prasad, J. Am. Chem. Soc. **121**, 5287 (1999).
[10] K. Roy Choudhury, Y. Sahoo, and P. N. Prasad, Adv. Mater. (Weinheim, Ger.) **17**, 2877 (2005).
[11] K. Roy Choudhury, Y. Sahoo, S. Jang, and P. N. Prasad, Adv. Funct. Mater. **15**, 751 (2005).
[12] X. Li, J. W. M. Chon, and M. Gu, Aust. J. Chem. **61**, 317 (2008).
[13] X. Li, J. Van Embden, J. W. M. Chon, R. Evans, and M. Gu, Appl. Phys. Lett. **96**, 253302 (2010).
[14] J. G. Winiarz, L. Zhang, M. Lal, C. S. Friend, and P. N. Prasad, Chem. Phys. **245**, 417 (1999).
[15] D. J. Binks, S. P. Bant, D. P. West, P. O'Brien, and M. A. Malik, J. Mod. Opt. **50**, 299 (2003).
[16] F. Aslam, D. J. Binks, M. D. Rahn, D. P. West, P. O'Brien, and N. Pickett, J. Mod. Opt. **52**, 945 (2005).
[17] F. Aslam, D. J. Binks, M. D. Rahn, D. P. West, P. O'Brien, N. Pickett, and S. Daniels, J. Chem. Phys. **122**, 184713 (2005).
[18] S. Kim, B. Fisher, H. J. Eisler, and M. Bawendi, J. Am. Chem. Soc. **125**, 11466 (2003).
[19] S. A. Ivanov, A. Piryatinski, J. Nanda, S. Tretiak, K. R. Zavadil, W. O. Wallace, D. Werder, and V. I. Klimov, J. Am. Chem. Soc. **129**, 11708 (2007).
[20] C. Y. Chen, C. T. Cheng, C. W. Lai, Y. H. Hu, P. T. Chou, Y. H. Chou, and H. T. Chiu, Small **1**, 1215 (2005).
[21] J. van Embden and P. Mulvaney, Langmuir **21**, 10226 (2005).
[22] B. Blackman, D. M. Battaglia, T. D. Mishima, M. B. Johnson, and X. Peng, Chem. Mater. **19**, 3815 (2007).
[23] R. Xie, U. Kolb, J. Li, T. Bashe, and A. Mews, J. Am. Chem. Soc. **127**, 7480 (2005).
[24] J. van Embden, J. Jasieniak, and P. Mulvaney, J. Am. Chem. Soc. **131**, 14299 (2009).
[25] X. Li, C. Bullen, J. W. M. Chon, R. A. Evans, and M. Gu, Appl. Phys. Lett. **90**, 161116 (2007).
[26] E. Hendrickx, Y. Zhang, K. B. Ferrio, J. A. Herlocker, J. Anderson, N. R. Armstrong, E. A. Mash, A. P. Persoons, N. Peyghambarian, and B. Kippelen, J. Mater. Chem. **9**, 2251 (1999).
[27] W. E. Moerner, A. Grunnet-Jepsen, and C. L. Thompson, Annu. Rev. Mater. Sci. **27**, 585 (1997).